

Effect of EFO parameters on Cu FAB hardness and work hardening in thermosonic wire bonding

A. Pequegnat · C. J. Hang · M. Mayer ·
Y. Zhou · J. T. Moon · J. Persic

Received: 9 October 2008 / Accepted: 16 December 2008
© Springer Science+Business Media, LLC 2009

Abstract Effects of the electrical flame off (EFO) parameters on the hardness and work hardening properties of Cu free air balls (FABs) are reported and compared to those of Au. Cu FABs were characterised using an online deformability method that measures the insitu deformability of the Cu FAB and by traditional off-line Vickers microhardness testing of cross-sectioned samples. The online deformability measurements are about twice as precise as the microhardness measurements. Cu FABs produced using EFO current (I_{EFO}) and EFO time (t_{EFO}) of 250 mA and 0.118 ms, respectively, have 14.29 HV (21%) higher hardness than those produced with $I_{\text{EFO}} = 45$ mA and $t_{\text{EFO}} = 1.03$ ms. While the Cu FABs with $I_{\text{EFO}} = 250$ mA are the hardest, they are also the most deformable and end up the softest after bonding due to less work hardening than observed with lower I_{EFO} FABs.

1 Introduction

In the microelectronics industry there is a continuous push for higher performance and lower costs. The community

responds to these demands by developing low-cost packaging solutions for fine pitch, high input-output devices [1, 2]. Thermosonic wire bonding is the most common first level interconnection technology used in the microelectronics industry ([1, 3]). The progressing demands have caused the industry to consider Cu wire opposed to the commonly used Au wire. Relative to Au wire, Cu wire has superior electrical and thermal conductivities as well as higher tensile strength, elongation and an increased “ball neck” strength [1–3]. The higher strength of Cu allows for longer distances between the ball and crescent bonds because the wire is more resistant to “wire sweep” which meets today’s demand for miniaturization. In addition to the superior properties of Cu wire, it comes at a relatively lower cost than the conventional Au wire. However, there are drawbacks to Cu wire when compared to Au wire, delaying the replacement of Au wire. Cu is harder than Au and an oxide layer forms readily on its surface ([2, 3]). Cu wire requires a higher bonding force and higher ultrasonic (US) levels. This causes an increase in the likelihood of underpad damage such as pad cracking or peeling and silicon cratering [3, 4]. In order to limit the oxidation the bonder must be retrofitted with a Cu package that consists of a means of supplying a shielding gas during bonding.

There are several different approaches in reducing underpad stress and therefore limiting damage during thermosonic bonding with Cu wire. Some approaches to reducing underpad damage are by using softer wire, producing softer free air balls (FABs), optimising the bonding parameters, and even by modifying the bond pad design [3–5]. Electrical flame off (EFO) parameters and the temperature of the shielding gas can be changed to produce Cu bonded balls [5] and Cu FABs [6] with different hardnesses.

A. Pequegnat (✉) · C. J. Hang · M. Mayer · Y. Zhou
Centre for Advanced Materials Joining, University of Waterloo,
Waterloo, ON N2L 3G1, Canada
e-mail: apequegn@uwaterloo.ca

C. J. Hang
State Key Laboratory of Advanced Welding Production
Technology, Harbin Institute of Technology, 150001 Harbin,
China

J. T. Moon
MK Electron Co. Ltd, Yongin, Korea

J. Persic
Microbonds Inc., Markham, ON, Canada

The microhardness of the bonded balls (BBs) has been investigated [5]. It was concluded that it decreases with increasing I_{EFO} with t_{EFO} adjusted to leave the FAB diameter constant. The amounts of US effects and work hardening were not discussed. Possible US effects include acoustic softening and residual hardening that have both been observed in metals that are subject to US energy [7].

In the current study the effects of EFO parameters on the hardness of FABs are examined. By performing manual microhardness tests and an online deformability study [8] the FAB is characterised before bonding takes place. This eliminates the US effect from the experiment.

2 Experimental procedure

The wires selected for this study are standard 25 μm diameter Au and Cu wires manufactured by MK Electron Co. Ltd., Yongin, Korea. The basic mechanical properties are outlined in Table 1. The wire Vickers hardness is measured on cross-sections orthogonal to the wire axis.

EFO parameters are determined that will produce $50 \pm 1.0 \mu\text{m}$ diameter FABs for both the Au and Cu wires. In order to find these parameters a total of 30 FABs are measured using three different EFO times (10 FABs for each EFO time) while holding the other EFO parameters constant. A shielding gas of 5% $\text{H}_2 + 95\% \text{N}_2$ with a flow rate of 0.5 L/min is used for Cu wire bonding to prevent the oxidation of the molten Cu during EFO [8]. The Cu FABs are examined using a Joel JSM-6460 scanning electron microscope (SEM) to ensure the flow rate of the shielding gas is sufficient to prevent oxidation during EFO. Figure 1 shows a 50 μm Cu FAB with no oxidation, observed under the SEM. The FAB diameters are measured using an optical microscope and fitted to a second order polynomial as shown for the Cu wire at the high I_{EFO} level in Fig. 2 [4]. This method is performed for each of the low, medium and high I_{EFO} of 45 mA, 80 mA, and 250 mA, respectively. The I_{EFO} , t_{EFO} and the average FAB diameters obtained are presented in Tables 2 and 3 for Cu and Au wires, respectively. For a 50 μm FAB produced with $I_{EFO} = 45 \text{ mA}$, the t_{EFO} for Cu is 44% larger than that required for Au. The difference is possibly due to the superior thermal conductivity of Cu. However, as I_{EFO} is increased the difference in the required t_{EFO} between the Cu wire and Au wire decreases. At an I_{EFO}

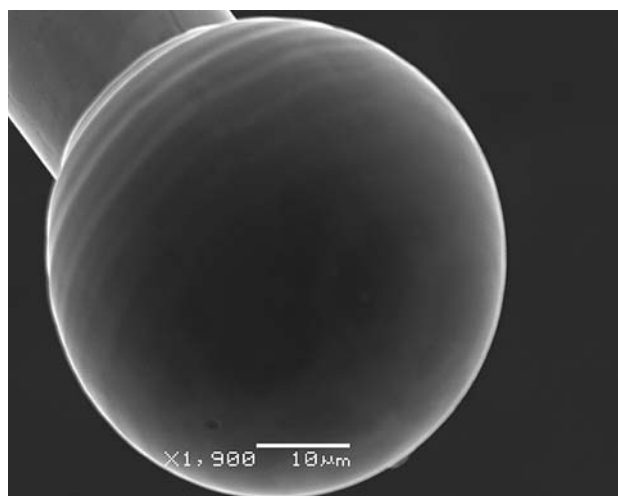


Fig. 1 SEM image of 50 μm Cu FAB (no oxidation observed)

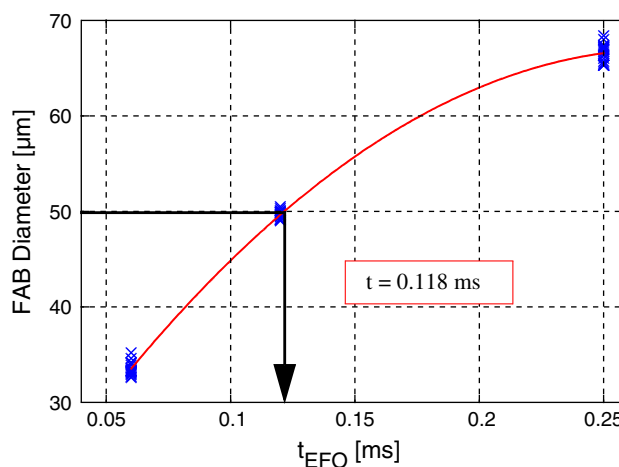


Fig. 2 FAB Diameter vs. t_{EFO} for Cu. Solid line represents polynomial curve fit. $I_{EFO} = 250 \text{ mA}$

of 250 mA the t_{EFO} required for the Cu FABs is only about 7% larger than that for the Au FABs. Possibly, the rate and magnitude of heat input is large enough at higher current levels to render the heat conducted away through the wire insignificant.

The online deformability test [8] was performed using an automated ESEC 3100 thermosonic wire bonder, manufactured by Oerlikon ESEC, Cham, Switzerland. An encoder measures the bondhead position with sub-micron precision along the z-axis. The z-position of the capillary

Table 1 25 μm (1 mil) diameter wire properties

Property	Cu	Au
Minimum breaking load (mN)	49	98
Elongation (%)	4–18	2–8
Vickers hardness	57.8	50.0

Table 2 Cu EFO parameters and resulting FAB sizes

Cu	Low current	Medium current	High current
EFO current (mA)	45	80	250
EFO time (ms)	1.03	0.43	0.118
Avg. FAB diameter (μm)	49.64 ± 0.44	49.74 ± 0.53	49.74 ± 0.38

Table 3 Au EFO parameters and resulting FAB sizes

Au	Low current	Medium current	High current
EFO current (mA)	45	80	250
EFO time (ms)	0.58	0.3	0.11
Avg. FAB diameter (μm)	49.98 ± 0.42	49.99 ± 0.48	50.27 ± 0.73

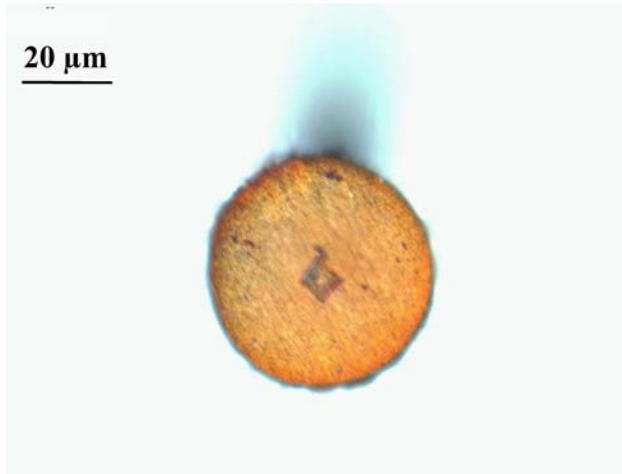


Fig. 3 Cross-section of a Cu FAB with Vickers hardness indentation

tip is derived from this encoder measurement and recorded during bonding. These signals are used to determine the deformed ball height (BH). The deformed BH is representative of the deformability of the initial FAB [8]. The deformability depends on material hardness and work hardening. FABs produced using low, medium, and high I_{EFO} are deformed using a deformation force of 0.6 N.

The next step is to compare the online deformability results to microhardness measurements made in the centre of the polished cross-sections of FABs as shown in Fig. 3 and in the centre of the cross-sections of BBs as shown in Fig. 4. The hardness measurements were performed using a

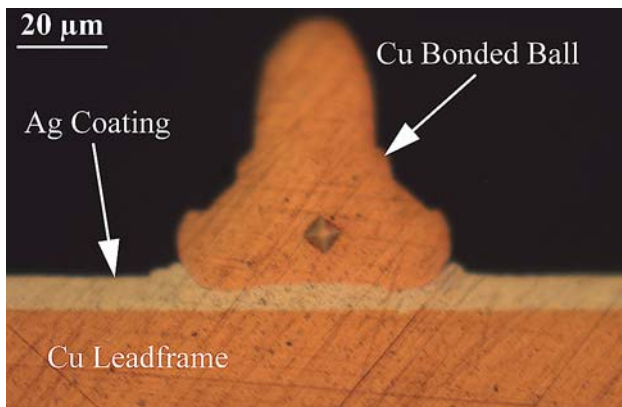


Fig. 4 Cross-section of a Cu BB with a Vickers hardness indentation

LECO DM-400LF hardness tester with Vickers indenter applying a 49 mN (5 gf) load with a 15 s dwell time. The measurements were made using an optical microscope and the vickers hardness was calculated using

$$HV = \frac{1854.4 \times P}{d^2}$$

where P is the applied load in gf and d is the average length in μm of the two diagonals measured from the microhardness indentation [9].

3 Results and discussion

3.1 Online deformability

Deformability results are shown in Fig. 5, where the BH decreases as the EFO current increases. The average BHs and their associated errors are shown in Table 4 for both Au and Cu at each of the I_{EFO} levels. The amount of deformation increases with increasing the I_{EFO} for both Au and Cu.

The online deformability results are consistent with BB microhardness results [5], which were subject to US energy. Both the online deformability study and [5] suggest that FABs produced with a higher I_{EFO} and lower t_{EFO} will have a lower hardness. However, no conclusion regarding

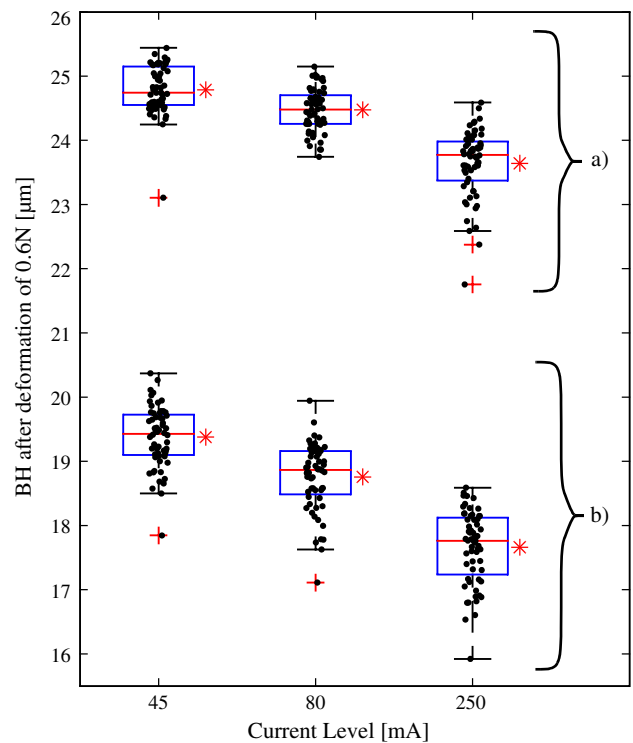


Fig. 5 Online deformability results for Au and Cu 50 μm diameter FABs. **a** Cu BH after deformation, **b** Au BH after deformation. Mean values are represented by star symbols

Table 4 Average BHs and error values from online deformability study

	Current level		
	45 mA	80 mA	250 mA
Au BH (μm)	19.38 ± 0.06	18.76 ± 0.07	17.66 ± 0.07
Cu BH (μm)	24.79 ± 0.05	24.48 ± 0.04	23.64 ± 0.07

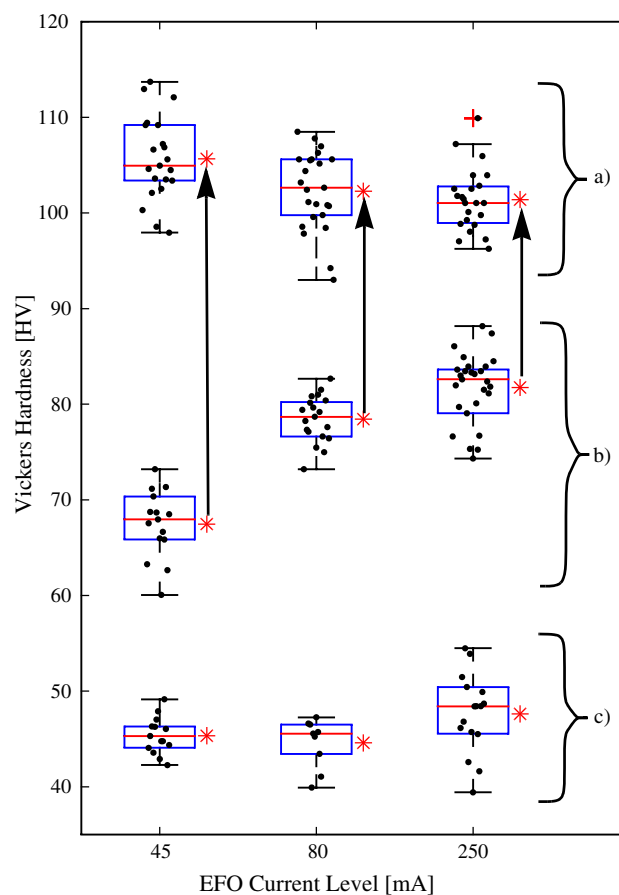
the FAB hardness before deformation can be made yet. For this, the amount of work hardening needs to be characterised.

3.2 Free air ball (FAB) microhardness

During EFO, the wire end is heated until molten into a droplet of desired diameter. The longer t_{EFO} , the more the wire adjacent to the droplet is heated, resulting in a larger heat affected zone (HAZ). While heat is radiated and convected to the atmosphere, the main driver for the solidification after EFO is the heat conducted to the un-molten wire [10].

In the case of the higher I_{EFO} value coupled with the shorter t_{EFO} , it is expected that the droplet peak temperature is higher [5], followed by higher cooling rates and gradients. The resulting FAB is expected to have a higher residual stress, dislocation density, and therefore hardness.

The Cu FAB microhardness results presented in Fig. 6 and Table 5 confirm this reasoning. Cu FABs produced with the lower I_{EFO} (45 mA) have a substantially lower microhardness (14.29HV lower) than that of FABs produced with the higher I_{EFO} (250 mA). However, considering the Au FAB results in Fig. 6 and Table 5, there is no significant hardness difference with the Au FABs as shown by the t -test results in Table 6. This might be due to the fact that between FAB solidification and microhardness testing, the FABs are subject to elevated temperatures. Bond-offs are made to a 220 °C hot substrate with the FABs hanging at the wire ends less than 0.5 mm away from the substrate. Therefore, the FABs remain at an elevated temperature for more than 20 min before the substrate is removed from the wirebonder hot plate. The FABs further experience elevated temperatures during the preparation steps for the microhardness test. The recovery and recrystallization temperature range for pure Au is between 150 and 200 °C [11], but highly deformed Au has even been observed to recover and recrystallize at room temperature ([11, 12]). Dopants are added to the Au wire to increase the annealing temperature and improve the thermal properties of the Au wire ([11, 13]). Even though dopants have been added, some recovery and recrystallization in the Au FAB may have occurred resulting in no change in microhardness at the different I_{EFO} levels.

**Fig. 6** Vickers hardness results: **a** Cu BB, **b** Cu FAB, **c** Au FAB. Mean values are represented by star symbols**Table 5** Average FAB and BB vickers hardness and error values

	Current level		
	45 mA	80 mA	250 mA
Au FAB (HV)	45.34 ± 0.53	44.59 ± 0.91	47.63 ± 1.07
Cu FAB (HV)	67.46 ± 0.95	78.45 ± 0.58	81.75 ± 0.71
Cu BB (HV)	105.66 ± 0.98	102.27 ± 0.85	101.39 ± 0.71

Table 6 Student's t -test results for Au FAB vickers hardness

t -test comparison	P -value
Low I vs. medium I	0.4355
Medium I vs. high I	0.0579
Low I vs. high I	0.0688

The relation of microhardness of the Cu FAB with the I_{EFO} level has the opposite trend of what was found for the BBs hardness in [5] and in the online deformability study

(Fig. 5). This opposite trend suggests different amounts of work hardening on the FABs when produced with different process conditions. The work hardening effect during deformation is larger for Cu FABs produced at lower I_{EFO} levels. The FABs have a lower microhardness but deform relatively less during the online deformability test. The opposite trend observed could possibly be explained by different residual stresses in the FABs. The residual stresses in the FAB produce local back stresses according to the Bauschinger effect [14]. These back stresses will aid in the movement of dislocations in the opposite direction of the original stress that caused dislocation motion, making deformation easier and reducing work hardening under deformation [14]. Therefore, FABs produced with higher I_{EFO} are more deformable.

3.3 Bonded ball (BB) microhardness

The microhardness of cross-sectioned Cu BBs with respect to the I_{EFO} level, shown in Fig. 6 and Table 5 follow the same trend as the microhardness results in [5] and the online deformability test (Fig. 5). The BBs that are produced with a higher I_{EFO} level FAB have a lower hardness than BBs that are produced using a lower I_{EFO} . The observed difference in microhardness of the Cu BBs produced using $I_{EFO} = 45$ mA and $I_{EFO} = 250$ mA is 4.27 HV. A difference of 9.28 HV was observed between BBs produced using FABs using $I_{EFO} = 30$ mA and $I_{EFO} = 105$ mA in [5].

The difference between the change in hardness in this study compared to [5], possibly is due to US effects. In the current study an ultrasonic generator current (USG) of approximately 590 mA was used where as [5] used an USG current of only 90 mA. Even if the USG current values obtained from two different wire bonder types cannot be directly compared, the BBs in the current study were severely overbonded compared to those in [5]. More US will result in larger effect on the mechanical properties of the BB. The higher level of US used in this study will diminish the effects of varying I_{EFO} during FAB formation. The amount of hardening related to strain hardening or ultrasonic effects cannot be distinguished between in this study.

In order to reduce the underpad stress that can cause underpad damage during bonding, more than the hardness of the Cu FAB should be considered. The EFO parameters that affect the hardness of the FAB also effect the magnitude of work hardening that occurs during bonding. The harder FAB produced at a high I_{EFO} will produce a softer BB relative to softer FABs that are produced with lower I_{EFO} . Therefore, a harder Cu FAB will be more desirable because it will work harden less, producing a softer deformed ball and reduces die pad stresses during subsequent bonding [15].

Table 7 Percent error of difference for online deformability and vickers hardness method

Cu wire I_{EFO} comparison	% Error of difference	
	Online deformability	Vickers hardness
Low vs. medium	21.3	38.3
Medium vs. high	9.8	126.1
Low vs. high	7.5	28.3

3.4 Comparison of testing methods

The results obtained from both the online deformability test and the Vickers hardness test show that Cu FABs produced with higher I_{EFO} will be relatively softer either, after being deformed using the online method or, both deformed and bonded when using the Vickers hardness method.

Since, both of the methods give similar trends with respect to the level of I_{EFO} , a correlation between the results can be obtained. Using the averages for each I_{EFO} level from both of the methods the correlation coefficient is calculated to be $r = 0.83$. The US effects experienced by the BBs may be responsible for weakening the correlation between the two methods.

In order to determine which method of measuring hardness is more precise the error of the differences between the mean values at each I_{EFO} level is taken. The percentage of the error of difference is a measure for the precision of the test method. The percentages of the error of difference are outlined in Table 7 for both the online and Vickers hardness methods. The online method when comparing the difference between the low vs. medium I_{EFO} , medium vs. high I_{EFO} , and low vs. high I_{EFO} is therefore approximately 2 times, 12.5 times, and 4 times, respectively, more precise than the Vickers hardness method. There is naturally more error built into the Vickers hardness method, as error can arise from specimen preparation and mounting, inadequate optical measurements or even by the effects of the specimens structure [9]. The second factor affecting the accuracy is that the US effect which, is not present during the online deformability test. The US effect does, however, become a factor when performing the Vickers hardness test on the Cu bonded balls and may be responsible for adding additional error to the microhardness results.

4 Conclusions

While no significant effect of EFO parameters on the microhardness of Au FABs was observed, it has been shown that the EFO parameters have a substantial effect on

Cu FABs. Upon initial deformation as typically observed in microelectronic ball bonding, work hardening occurs for both materials and depends on EFO parameters in a similar way for both materials. The work hardening effect is stronger with FABs produced with lower I_{EFO} levels, completely compensating for the difference in hardness that exists before deformation. These results contribute to an improved understanding of FAB formation and deformation effects which are affecting the US stress levels present during the bonding process. Such understanding can help find a way how to reduce the underpad damage in Cu ball bonding processes on sensitive substrates.

Acknowledgments This work is supported by the Natural Science and Engineering Research Council (NSERC) of Canada, Microbonds Inc., Markham, Canada, and MK Electron Co. Ltd., Yongin, Korea. Technical discussions with Dr. Jaesik Lee are greatly appreciated.

References

1. W.J. Greig, *Integrated Circuit Packaging, Assembly and Interconnections* (Springer Science + Business Media LLC, 2007)
2. Y. Zhou, *Microjoining and Nanojoining* (Woodhead Publishing Ltd., Cambridge, England, 2008)
3. G. Harman, *Wire Bonding in Microelectronics Materials, Processes, Reliability, and Yield*, 2nd edn. (McGraw-Hill, New York, 1997)
4. A. Shah, M. Mayer, Y. Zhou, S.J. Hong, J.T. Moon, Reduction of Underpad Stress in Thermosonic Copper Ball Bonding, in proceedings of the 58th Electronic Components and Technology Conference (2008), p. 2123–2130
5. Z.W. Zhong, H.M. Ho, Y.C. Tan, W.C. Tan, H.M. Goh, B.H. Toh, J. Tan, *Microelectron. Eng.* **84**, 368–374 (2007)
6. J. Onuki, M. Koizumi, H. Suzuki, *J. Appl. Phys.* **68** (II) (1990) 5610–5614
7. B. Langenecker, *IEEE. Trans. Sonics. Ultrason* **SU-13**, No. 1, 1–8 (1966)
8. C.J. Hang, I. Lum, J. Lee, M. Mayer, C.Q. Wang, Y. Zhou, S.J. Hong, S.M. Lee, *Microelectron. Eng.* **85**, 1795–1803 (2008)
9. J.H. Westbrook, H. Conrad, *The Science of Hardness Testing and Its Research Applications* (American Society for Metals, ASM, Ohio, 1973)
10. C.J. Hang, C.Q. Wang, Y.H. Tian, M. Mayer, Y. Zhou, *Microelectron. Eng.* **85**, 1815–1819 (2008)
11. J.H. Cho, J.S. Cho, J.T. Moon, J. Lee, Y.H. Cho, Y.W. Kim, A.D. Rollet, K.-H. Oh, *Metallurg. Mater. Trans.* **34A**, 1113–1125 (2003)
12. *ASM Handbook Volume 2, Properties and Selection: Nonferrous Alloys and Special-Purpose Materials*, ASM International (1992)
13. G. Qui, S. Zhang, *J. Mater. Process. Technol.* **68**, 288–293 (1997)
14. E. Orowan, Internal stress and Fatigue in Metals, *Proc. Internal Stresses and Fatigue in Metals*, Detroit and Warren, Michigan 1958 (Edited by G.M. Rassweiler and N.L. Grube) p.59, Elsevier, London (1959)
15. A. Shah, M. Mayer, Y. Zhou, S.J. Hong, J.T. Moon, *Microelectron. Eng.* **85**, 1851–1857 (2008)